Scientific Research Publishing

Advances in Remote Sensing, 2025, 14(2), 87-102
https://www.scirp.org/journal/ars
ISSN Online: 2169-2688
ISSN Print: 2169-267X

Quantifying Temporal Distortions of Artificial UAV Crop Canopy Temperature Measurements

Timothy S. Goebel, James R. Mahan, Paxton Payton, Andrew Young, N. Ace Pugh, Zhanguo Xin, John E. Stout, Robert J. Lascano*

USDA-ARS, Cropping Systems Research Laboratory, Lubbock, TX, USA
Email: *Robert.Lascano@usda.gov

How to cite this paper: Goebel, T.S., Mahan, J.R., Payton, P., Young, A., Ace Pugh, N., Xin, Z.G., Stout, J.E. and Lascano, R.J. (2025) Quantifying Temporal Distortions of Artificial UAV Crop Canopy Temperature Measurements. *Advances in Remote Sensing*, **14**, 87-102.
https://doi.org/10.4236/ars.2025.142006

Received: May 21, 2025
Accepted: June 27, 2025
Published: June 30, 2025

Abstract

The crop canopy temperature (T_c) measured with fixed-infrared thermometers (IRT's), provides high-resolution data but only measures small areas of the canopy. Conversely, thermal sensors mounted on UAVs measure T_c over larger areas, overcoming this limitation. However, these measurements may introduce distortions of T_c's values due to the time of day when they are measured. We measured T_c of a cotton crop over a growing season using fixed-IRTs and compared these measurements to the same data with an assumed time delay of 0.25 - 2 hours. This delay was used as a proxy of T_c values measured with a UAV. The dataset consisted of 7 IRTs measuring 96 values/day over 67 days. Results showed that artificial UAV flight missions resulted in a thermal distortion related to the flight duration. This distortion was applied to detect differences of T_c in seven irrigation treatments. The difference in T_c from the UAV and fixed IRT was affected by the time of day, irrigation treatment, and UAV-flight duration. To identify irrigation treatments, the assumed UAV-T_c produced up to 27% spurious treatment differences relative to the fixed-IRT. Distortion in UAV-T_c was minimal for flights of <15-minutes. Interpretation of UAV-T_c data should consider this distortion.

Keywords

Fixed-Infrared Thermometer (Fixed-IRT), Irrigation Treatment, Thermal Distortion

1. Introduction

The use of plant temperature as an indicator of metabolic status has been used for more than 25 years [1]-[6]. Transpiration alters the temperature of the leaves [1] [3] and this temperature change can be measured continuously under a variety of

conditions in a non-destructive and reproducible manner [2] [6].

In agricultural settings, the crop canopy temperature (T_c) is often measured with infrared thermometers (IRT) placed among the plants in a field. These stationary IRT sensors are referred to herein as "fixed-IRTs". While fixed-IRTs measure data with high temporal resolution, *i.e.*, 15-minute data across the growing season, they are stationary and generally have a spatial resolution of <0.5 m^2. Given this limitation, there is an interest in increasing the spatial resolution by moving the sensor throughout the field either by walking with a handheld version of the instrument, attaching a sensor to a vehicle, or using a small Unmanned Aerial Vehicle (UAV). These platforms can provide the necessary spatial coverage and resolution; however, they are limited in their ability to collect repeated measurements, resulting in reduced temporal resolution [7]-[9]. Small unoccupied aircraft systems can be equipped with a variety of sensors including red, green, blue cameras (RGB), multispectral sensors, and thermal sensors [10]. Although many studies have used RGB and multispectral sensors, few studies have investigated best practices for the use of thermographic imagery collected by a UAV. Beyond the inherent difficulties involved in calibrating thermographic imagery, it is also crucial that parameters outside of the UAV or its payload be considered, e.g., the weather conditions and the altitude of the flight [11] [12]. Further temporal considerations, such as the time of day and differentials in temperature from the beginning of a flight mission to the end, are also important factors when designing thermal flight missions that have not been evaluated [12]. A small UAV equipped with thermal sensors offers researchers and producers the ability to monitor T_c over many hectares at daily intervals [13]-[16].

With regard to irrigation, one must consider two important factors: when to irrigate and how much water to apply. The frequency of irrigation depends on the availability of irrigation-water and the amount to apply depends on the demand, a function of the environment and crop growth stage. Past research has addressed the different methods to measure and calculate crop evapotranspiration (ET) over the length of the growing season [17]-[19]. Examples of these measurements include field lysimeters [20] [21], stem flow gauges [22], water-balance by measuring soil water content as a function of depth and time, among other methods. A commonly used technique to calculate crop ET is the so-called "engineering method", first proposed by Jensen [23] and discussed by Lascano [24]. This method provides an hourly or daily estimate of reference crop ET, for either a short or a tall crop, using the well-known Penman-Monteith equation and a crop-specific coefficient to calculate a corresponding crop ET [25]. Another well-known method is the Crop Water Stress Index (CWSI), used to calculate the relative transpiration rate of the plants at the time of measurement and is calculated from measurements of the T_c and vapor pressure deficit [26] [27]. A variant of CWSI, called BIOTIC, uses T_c and time thresholds to determine when to irrigate and how much water to apply [28]. Regardless of the method used, it is apparent that both measurements and calculations of crop ET require meteorological sensors that are expensive and

require maintenance to manage the daily water requirement of a crop. However, this management scheme is not practical for large field applications. An alternative method is the use of a UAV equipped with a variety of sensors, *i.e.*, RGB, multispectral and thermal, that can cover large fields. Furthermore, the cost of this technology continues to decline as smaller and more cost-effective hardware becomes available. For example, an orthoimage developed from a UAV flight can be assembled from hundreds of individual images in a manner that does not retain information regarding the time of measurement. The temperature data in an orthoimage is measured on a per pixel value and the assembly of the orthoimage uses software that does not provide any of the associated metadata (timestamp) of the assembled pixel. Without the timestamp of when the pixel was taken it is therefore difficult to determine the corresponding values of air temperature, humidity, wind speed and global irradiance that are needed to calculate values of crop ET, CWSI, etc. that change with time. In this paper we support the use of UAVs to measure the necessary data to calculate crop ET but suggest that some of the drawbacks need to be considered, which are often ignored when extracting data from thermal orthomosaics.

Replacing fixed-IRTs with mobile platforms will reduce the number of measurements made per day. For example, using a single sensor and moving it in the field will require a large investment of time because the user must move between sampling locations and the elapsed time can range from seconds (UAV measurements) to minutes (ground measurements). In an agricultural setting, measurements of T_c will be made in an environment where the T_c is continuously changing. Given that the results from moving a sensor around a field is to evaluate the field spatially and not temporally, care must be taken to ensure that diurnal changes in T_c do not artificially distort the spatial measurements. Given this limitation, it was of interest to evaluate the maximum amount of time between two T_c measurements before the measurements can no longer be compared spatially due to temporal T_c changes. To address this issue, the objectives of this study were to: 1) artificially change the T_c occurring between the thermal measurements captured at different time intervals using a UAV-thermal platform as the basis for comparison in an agricultural setting, and 2) use data from an irrigation treatment experiment to artificially generate canopies with different crop water status from no irrigation to an application of 6 mm/d.

2. Materials and Methods

2.1. Overview of Approach

For this study, we used archived T_c data from an irrigation experiment conducted in 2009 that were temporally distorted in silico and then compared to the original T_c values. The data consisted of T_c measurements recorded in 15-minute intervals collected from seven irrigation treatments (ranging from 0 to 6 mm/d) over the course of 67 days [27]. These original T_c data were used to evaluate how often all seven treatments were distinguished from each other. Additionally, the data were

offset by time (ranging from 15 to 120 min) to recreate the changes in T_c that would occur over different UAV-thermal mission flight durations. In the context of this study, we introduced an artificial UAV-T_c measurements as a proxy dataset of T_c values to evaluate the temporal effect. The benefit of T_c data in 15-minute intervals is that T_c is determined with a high degree of precision over time. For this study, we assumed that this would approximate a UAV having imaged that small portion of the field where the sensor was located in similar 15-minute intervals. Therefore, it was possible to offset the time course of the T_c data to artificially generate images collected using a UAV that occurred 15, 30, 45, 60, 90 and 120 minutes later. These data were then analyzed to examine the effect of flight duration on T_c differences across the 7 irrigation treatments. In addition, this analysis allowed for the accurate quantification of temporal differences in crop water status. Using the T_c data in this fashion allowed for the creation of a T_c dataset to which deviations could be compared. For the purposes of this study, these data are referred to as "Standard T_c". These Standard T_c data had high temporal resolutions which would have been difficult to obtain using a UAV-based thermal imaging system alone.

2.2. Plot Characteristics

The continuous data were collected in 2009 at the Texas Tech University Research farm in Lubbock, TX [27]. Cotton (DeltaPine 147RF, Monsanto, St. Louis, MO, USA) was planted on 15 May 2009, Day of Year (DOY 135). The soil of all sampled plots is classified as an Amarillo soil series (fine-loamy, mixed, superactive, thermic Aridic Paleustalfs). Agronomic practices were in accord with regional norms. Irrigated plots ~ 0.20 ha in size (4 rows × 10 m length) were watered with a subsurface drip irrigation system with one irrigation line/row. Drip irrigation lines were placed 0.20 m below the planted rows, which were 1-m apart. Plots were irrigated daily beginning 53 days after planting for 67 days from DOY 188 to DOY 264 with the following amounts: 1, 2, 3, 4, 5, and 6 mm.

2.3. Thermal Data Collection

The changes in T_c were measured with infrared thermometers (IRT) (SmartCrop™ Smartfield Inc., Lubbock, TX, USA) that were factory calibrated. One fixed-IRT was placed in each irrigation zone/irrigation treatment. The fixed-IRTs were positioned ~ 0.2 m above the plant canopy at a 60˚ oblique angle. Each fixed-IRT had a 1:1 view ratio with a 0.2 m height placement that corresponded to a 0.2-m radial view of the canopy, and the height and distance from the canopy were adjusted on a weekly basis. The measured changes in T_c from each fixed-IRT were collected at 1-minute intervals, and values were recorded as 15-minute averages. This resulted in 96 T_c measurements per day and per sensor across the 67-day study period from 11 July (DOY 192) 2009 to 15 September (DOY 258) 2009. In summary, the seasonal dataset for the seven fixed-IRTs consisted of 45,024 T_c values.

2.4. Artificial Generation of UAV-Based Temporal Offset

The thermal UAV offset temperatures were calculated using the T_c data. Thermal time separations were created by using the T_c measurements in the subsequent 15-minute period as the offset reading. This was done for 15-, 30-, 45-, 60-, 90-, and 120-minute thermal separations on the irrigation treatments 0-6 mm (Table 1). This method resulted in Standard T_c data and six UAV-thermal data sets of 15-, 30-, 45-, 60-, 90-, and 120-min flight durations.

2.5. Treatment Separation Events

In the dataset from [27], there were seven irrigation treatments that were combined into six irrigation treatment pairs for comparisons of T_c measurements over time. For each time point in the dataset, the irrigation treatment pairs consisted of T_c values for two irrigation treatments that differed in daily irrigation amount by 1 mm. Each treatment pair consisted of one lower irrigation treatment and one higher irrigation treatment, e.g., 0 mm/d and 1 mm/d. The lower irrigation treatment tended to have a higher T_c than the higher irrigation treatment. Differences in T_c value among treatment pairs were identified in a two-step process, as follows:

1) The difference (Δ) in T_c was calculated by subtracting the higher irrigation treatment from the lower irrigation treatment.

2) The T_c Δs were then converted to a binary format, where 1 indicated that the absolute value of Δ was > than 0.5˚C (the thermal resolution of the IRT) and a 0 indicated that the absolute value of the Δ was ≤0.5˚C.

The resulting binary data were used throughout the rest of the analyses as a simple way to differentiate between two treatments that were thermally distinct from each other at any given point in time. Thermal separations > 0.5˚C were considered a positive thermal separation; hereafter, referred to as treatment separation events (TSE). The TSEs were calculated for every time period during the 67-day study.

Table 1. Development of the artificial T_c dataset for UAV-thermal mission length. All data were collected on 12 July 2009 (DOY 193) at various times (hh:mm) of day. Letters (A~D) denote data used to develop the artificial dataset for further analysis. The bold and colored numbers in the "0 mm" column represent the initial value at Time 15:00 as indicated for other columns.

Time	Duration (min)	0 mm	0 mm - 30 min	0 mm - 60 min (B)	0 mm - 90 min (C)	0 mm - 120 min (D)
15:00	0	40.94	**40.37**	**40.13**	**38.46**	**38.41**
15:15	15	41.29	40.14	39.77	38.38	37.92
15:30	30	**40.37**	40.13	38.46	38.41	36.89
15:45	45	40.14	39.77	38.38	37.92	36.11
16:00	60	**40.13**	38.46	38.41	36.89	34.53
16:15	75	39.77	38.38	37.92	36.11	34.07
16:30	90	**38.46**	38.41	36.89	34.53	34.02
16:45	105	38.38	37.92	36.11	34.07	33.62
17:00	120	**38.41**	36.89	34.53	34.02	32.64
17:15	135	37.92	36.11	34.07	33.62	32.58
17:30	150	36.89	34.53	34.02	32.64	32.14
17:45	165	36.11	34.07	33.62	32.58	31.99

3. Results

The dataset used for analysis consisted of 45,024 values of measured T_c from seven fixed-IRT's in seven irrigation treatments over a 67-day study period. The measured T_c data were used to generate an additional 270,144 artificial T_c data that approximated typical UAV-thermal missions of varying duration. This set of measured and artificial T_c values, 315,168 measurements in total, were used in the analysis of the effect of differential irrigation on cotton T_c (Figure 1).

3.1. Reduction from 15-Minute to 1-Hour T_c Values during Daylight Hours

The goal of the study was to use T_c comparisons over time to identify irrigation responses in fixed-IRT data and to compare these results with those that could be obtained using the artificial UAV-thermal approach. A single UAV-thermal mission conducted per day during daylight hours was considered a reasonable goal for a field study. To recreate this daily mission, the dataset were reduced to hourly values for subsequent analyses. The primary approach was to perform the analysis in two sections:

1) in the first section, fixed-IRT data were analyzed regarding the ability for each to identify the irrigation treatment effects; and

2) the second section applies the same analysis to T_c data that were temporally offset to provide UAV-thermal recreations.

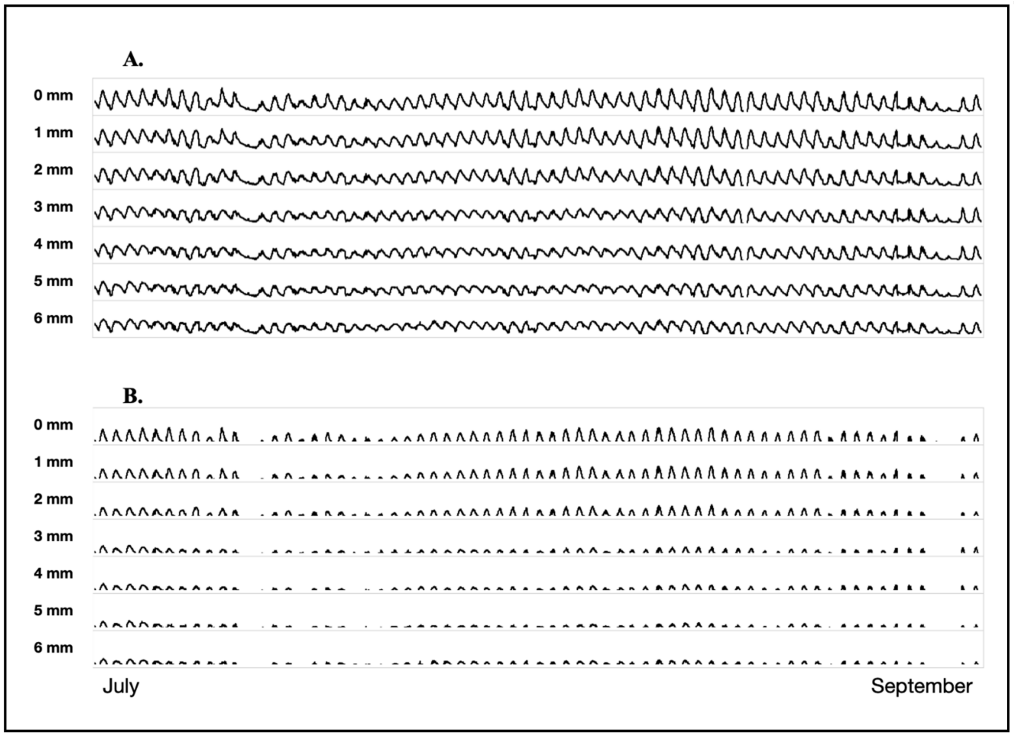

Figure 1. Canopy temperature during the 67-day study period measured every 15 minutes for the seven irrigation treatments. **(A)** The full-scale y-axis is 15˚C to 40˚C, **(B)** Canopy temperature is scaled to accentuate irrigation effects, and full-scale y-axis is 27˚C to 40˚C.

3.2. Analysis of Measured T_c from Fixed-IRT Sensors

3.2.1. Irrigation Treatment Pairs

The goal of this study was to detect differences among irrigation treatments based on T_c values. Seven irrigation treatments were grouped into six treatment pairs that represent 1 mm differences in daily irrigation amount. For example, the 0 mm/d and 1 mm/d irrigation treatments were paired to produce the 0 - 1 mm treatment pair. This produced the following irrigation treatment pairs; 0 - 1 mm, 1 - 2 mm, 2 - 3 mm, 3 - 4 mm, 4 - 5 mm, and 5 - 6 mm.

3.2.2. Treatment Separation Events

For each treatment pair at each interval, T_c data were compared to determine if they should be considered thermally separated. A separation for an irrigation treatment pair was defined as a T_c difference > 0.5˚C. For each comparison a TSE was assigned a value of 1 otherwise 0 was assigned according to the criteria described above.

With six treatment pairs over the 67-day study period, there were 402 treatment comparisons/hour in each day. The results of six treatment comparisons for each hour between 08:00 and 20:00 (13 hour/d) for the 67-day period are shown (Figure 2). For each day, at each hour, there are six treatment comparisons that could produce a maximum of six TSE for a total of 5226 treatment pair comparisons (6 treatment pairs × 13 hourly periods, × 67 days) (Figure 2).

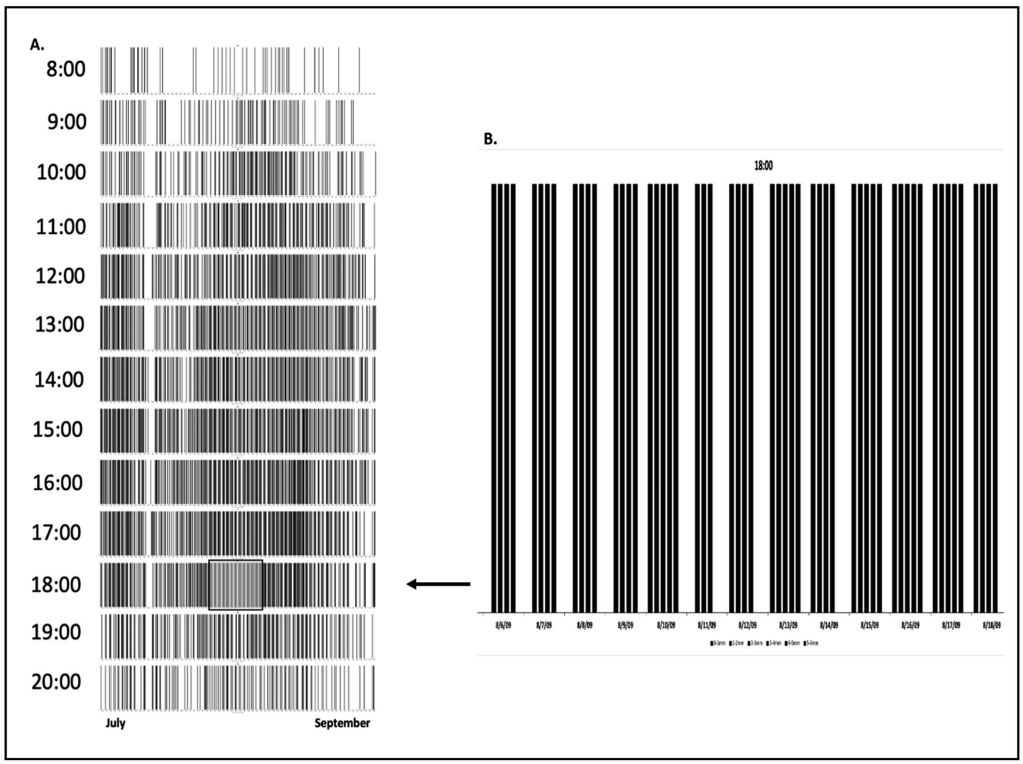

Figure 2. The hourly pattern of TSEs over 67 days for each day. There are six treatment pairs at each hourly measurement. Each TSE appears as a vertical mark. **Panel A** shows 67 days for 13 hours, and **Panel B** shows two weeks for 2 hours.

The pattern of TSE varied based upon the day and time of the measurement (Figure 2). The number of positive TSE across the daytime period decreased in the hours close to dawn and dusk, with the highest density of positive TSE occurring from 11:00 to 18:00 hours. Examined across the entirety of the study, there was some seasonality and weather influence present (Figure 2). There was a higher density of TSE at the beginning of the study in July 2009 as well as in the middle of August 2009 (Figure 2). The pattern of TSEs for each irrigation pair at 18:00 across the entire 67-day study period shows a general trend of decreasing TSEs with increasing irrigation volumes suggesting that irrigation treatments are more difficult to resolve at higher irrigation volumes (Figure 3). The number of TSEs for each treatment pair illustrates the decrease in TSEs with increasing daily irrigation volumes (Figure 4).

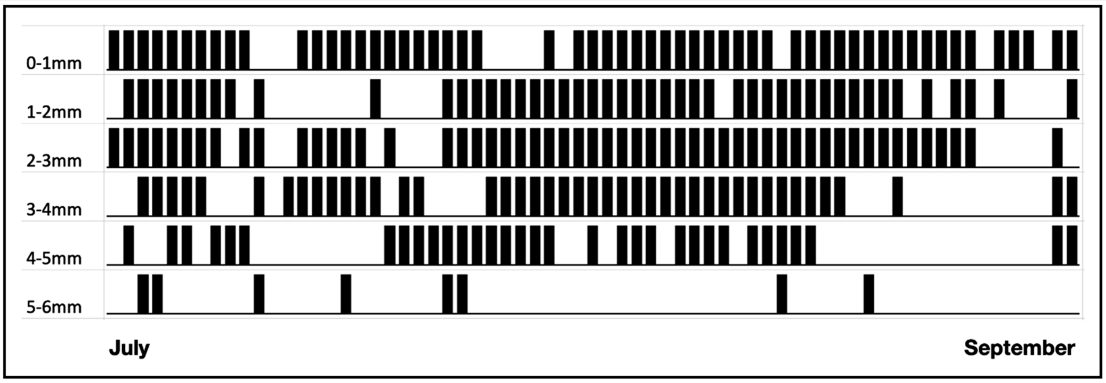

Figure 3. The 67-day pattern of TSEs at 18:00 hours separated by irrigation-treatment pair.

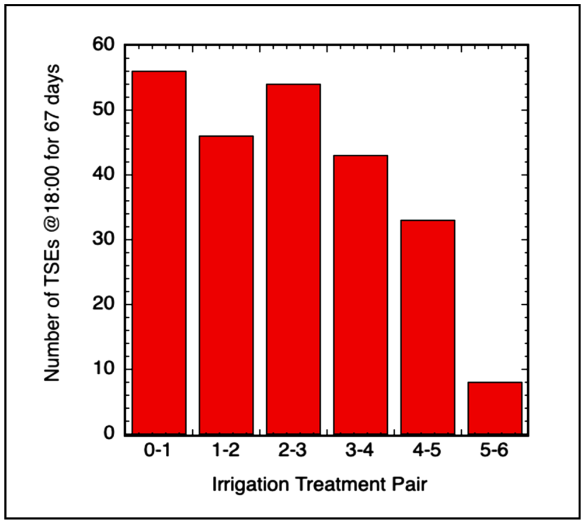

Figure 4. Number of TSEs for each irrigation treatment pair at 18:00 hours for 67-days of the study. The treatments differ by 1 mm/day of irrigation.

3.2.3. Identification of TSE Errors

The UAV-thermal distortion alters both the number of TSE observed and the T_c values associated with a given TSE. Treatment separation events were analyzed to

reveal the occurrence of spurious TSE that were artifacts of the artificial UAV-thermal method (Figure 5). Spurious TSEs were identified by comparing the pattern of TSEs in the fixed-IRT data with the TSE pattern in the artificial UAV-thermal data. Two types of TSE errors were identified: i) TSE deletions, where a TSE in the fixed-IRT data was not present in a UAV-thermal pattern, and ii) TSE additions, where a TSE in the artificial UAV-thermal data is not present in the fixed-IRT data. For the purposes of this study, TSEs that were added were designated as Type I errors and TSEs that were deleted were designated as Type II errors. The extremes were used to demonstrate the identification of TSE errors (Figure 5). The same analysis was applied across the collection of six treatment pairs for seven flight durations over 67 days at 18:00 hours.

In total, there were 2814 treatment pair comparisons resulting in 2161 TSE (Table 2). Of the 2161 TSE, 52 were Type II errors (2.4%) and 533 which were Type I errors (24.7%), resulting in 1680 true TSEs, *i.e.*, present in both the fixed-IRT and sUAS-thermal data. In the fixed-IRT (0 minute) data there are 240 total TSEs; thus, TSEs more than 240 are a result of the distortion associated with flight mission durations. In addition, the relative number of Type I errors increased as irrigation levels increased. As the irrigation amount increased, true TSEs decreased, and Type I errors increased (Figure 5). Evaluating daytime hours (8:00 - 20:00) across the 67-day period for the Standard T_c data as well as all artificial data clearly indicated a false reduction in TSEs with increasing flight time in the morning hours and a false increase in TSEs in the afternoon (Figure 6). Notably, the identification of the spurious TSEs was only possible because of the Standard T_c data that could be used for comparison, which would not be available in data collected solely with a UAV-thermal sensor.

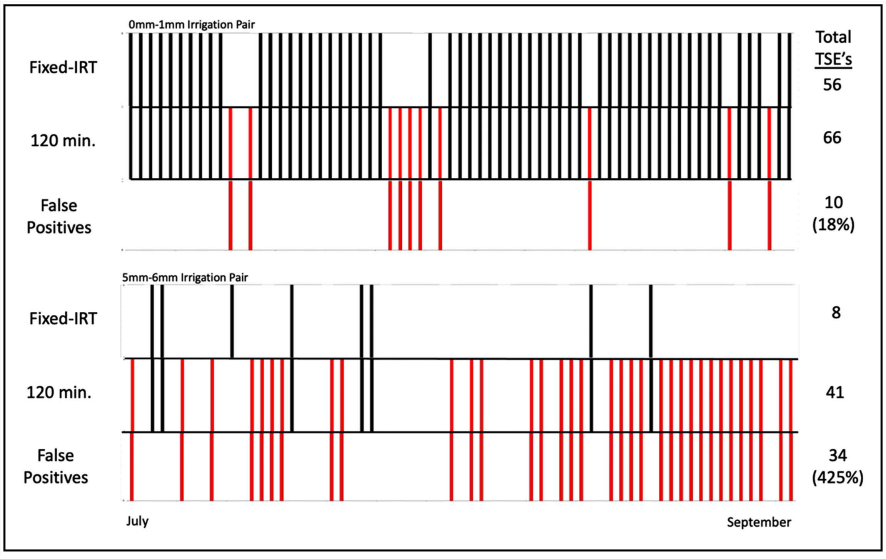

Figure 5. Graphical representation of the TSE errors throughout the 67-day period. The upper panel shows the 56 TSEs from the fixed-IRT, the middle panel shows 66 TSEs from a 120-minute artificial UAV thermal, and lower panel shows ten false positives TSEs unique to the 0 - 1 mm 120-minute data.

Table 2. Summary of the number of TSE for each UAV-thermal flight time and irrigation treatment pairs with a summary of Type I and Type II errors.

Irrigation Pairs	Fixed-IRT	15 min	30 min	45 min	60 min	90 min	120 min	Totals
0 - 1	56	59	63	64	64	66	66	
1 - 2	46	51	59	60	64	65	65	
2 - 3	54	58	62	63	63	65	65	
3 - 4	43	45	57	57	60	61	62	
4 - 5	33	40	48	55	52	48	51	
5 - 6	8	8	16	27	34	37	41	
# Possible Comparisons	402	402	402	402	402	402	402	2814
Total TSE	240	261	305	326	337	342	350	2161
# Type I Errors	N/A*	34	69	93	104	112	121	533
# Type II errors	N/A*	13	4	7	7	10	11	52

*by definition, there are no Type I errors.

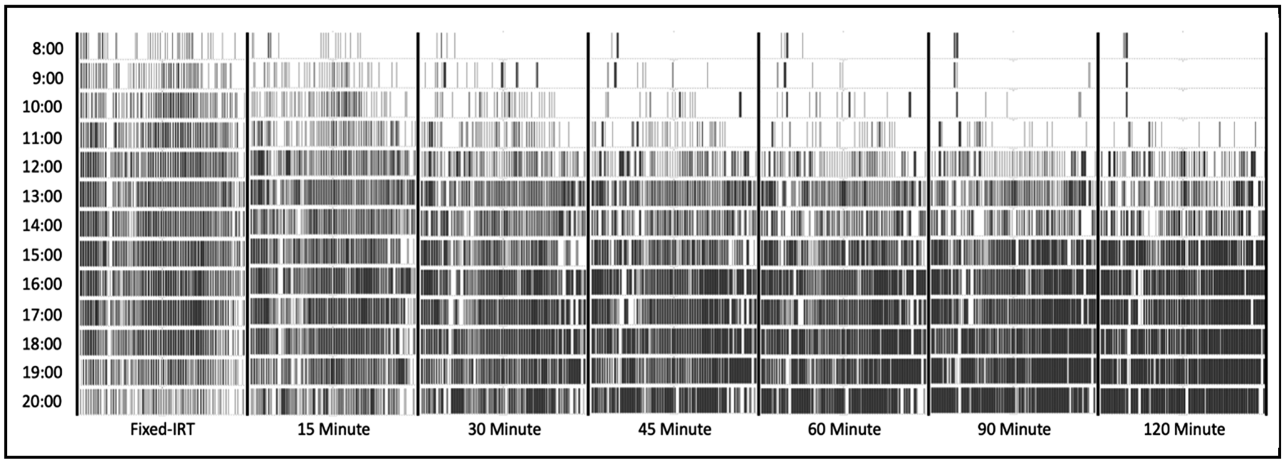

Figure 6. Full panel of TSE's from 8:00 to 20:00 hours across 67-days, including all thermal distortions for all irrigation treatments and UAV-thermal flight duration.

The effect of intermittent cloud cover during a thermal UAV flight was an additional point of concern in terms of contributing to Type I and Type II errors. Figure 7 depicts the presence of TSEs as vertical bars for each treatment pair across each hour from 8:00 - 20:00. At 13:00, shortwave solar irradiance was reduced to 568 W/m^2 and there were only two Type I errors in the lower irrigation treatment comparisons, however, there were nine Type II errors in the higher irrigation treatment comparisons. At 14:00 (solar noon at 13:50) there was a reduction in net solar irradiance suggesting that clouds interfered with solar transmission. During this period with clouds reducing the net solar irradiance there were no TSEs present in any of the irrigation treatments; however, the Fixed-IRT showed there should be thirty Type II errors. At 16:00 the solar irradiance dipped again; however, there were no errors generated in any of the treatment compari-

sons. Figure 7 suggests that the presence of intermittent cloud cover can create thermal artifacts in complex patterns that are difficult to identify.

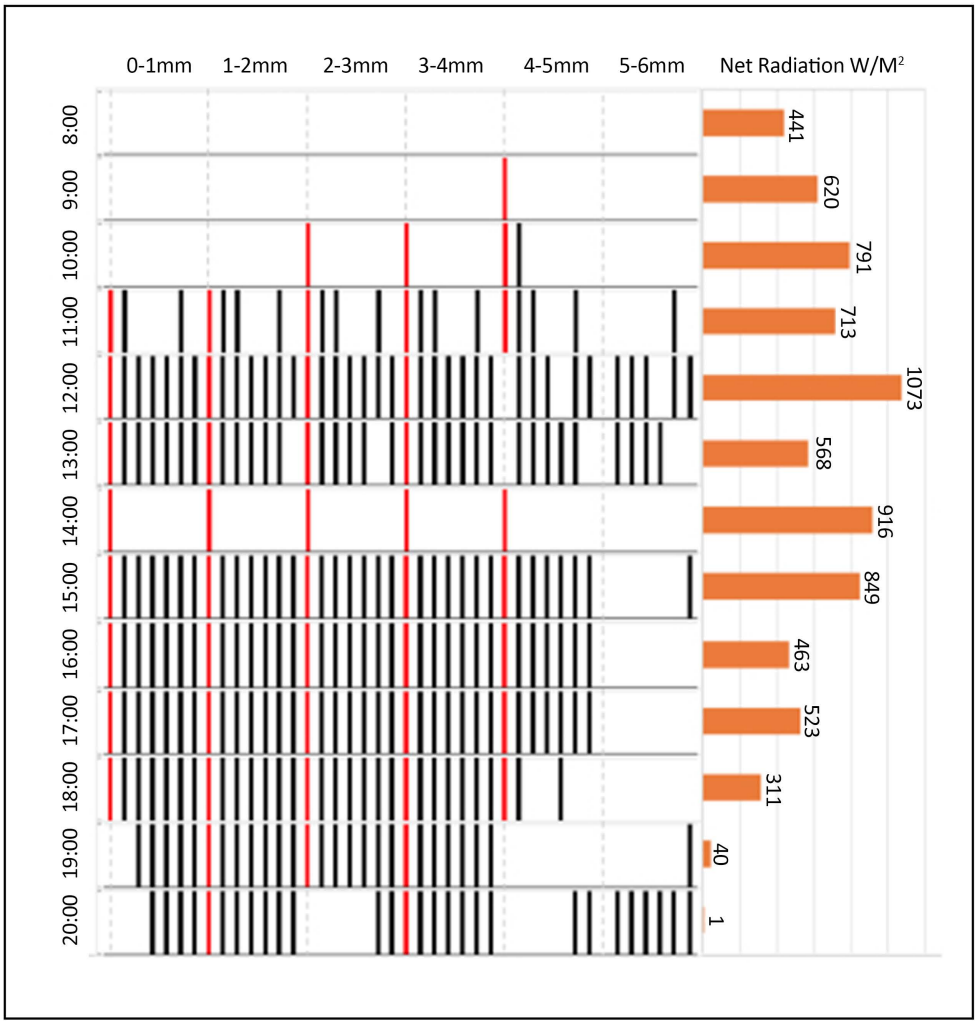

Figure 7. Effect of intermittent clouds on hourly TSEs for one day. The right panel is separated by treatment comparisons from 0 - 1 mm to 5 - 6 mm irrigation. Vertical bars denote a positive TSE, and red bars represent TSEs from the control (no shift in timestamp). The left side is the net solar radiation for the hour showing intermittent decreases due to clouds.

3.3. Mitigation of UAV-Based Thermal Distortion

The data presented in Table 2 suggests a relationship between the flight duration, measurement area and thermal distortion that can be described for a representative UAV-thermal mission (Figure 8). This artificial AV uses a flight coverage of 0.1 acres/minute (405 m^2/minute) at a flight height of 40 m [29]. The dashed line indicated the relationship between flight duration and measurement area. The thermal distortion associated with the UAV-thermal method is shown for each flight duration. Depending on what T_c distortion would be considered acceptable, a potential thermal UAV flight time could be restricted to as little as 30 minutes (0.5˚C).

4. Discussion

The purpose of this study was to compare the use of fixed-IRTs and UAV thermal sensors to detect differences among irrigation treatments in a cotton crop. The use of fixed-IRT sensors to detect differences in crop stress has been used in the past [2] [3]. The primary limitation of the fixed-IRT method is the reduced spatial footprint of the sensor. A UAV-thermal system has a much larger spatial footprint than a fixed-IRT sensor. A thermal artifact inherent in widely used UAV thermal approaches was explored in a previous study [30]. The TSE Type I error rate of 25% suggests there are potential complications that may arise when using UAV-based thermal methods. Regardless of the time of day or date that a flight mission is conducted, it appears likely that thermal distortion associated with the UAV method will be present.

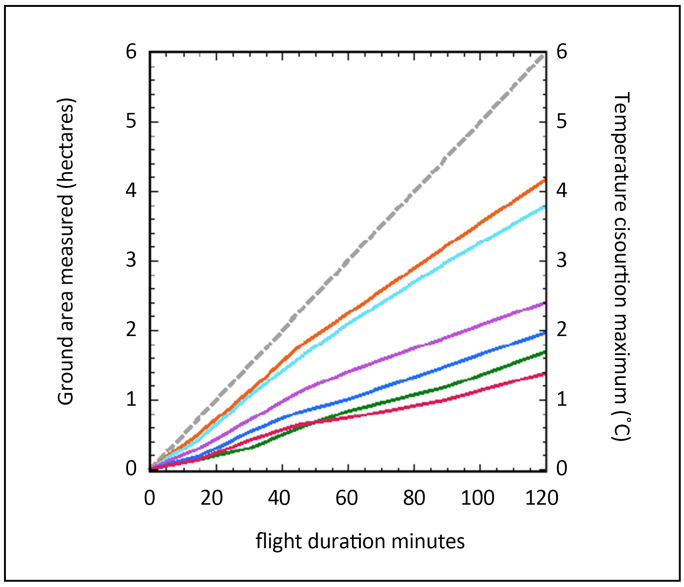

Figure 8. Ground area (ha) imaged in a UAV-thermal mission at a rate of 0.1 ha/minute as a function of the duration of the mission, which is shown by the dashed line. The colored lines represent the maximum thermal distortion in a UAV-thermal mission derived from temporal distortion of fixed-IRT data. Each line represents a different irrigation level.

In this study, fixed-IRT T_c data were used to create artificially time-shifted data from 15 minutes to 60 minutes and to explore how these time shifts change the resulting comparisons of irrigation treatments if it assumed that a time shift is not present. One of the potential drawbacks of this approach is that it does not provide a means to analyze the temporal distortion in UAV-thermal data. Thus, it is reasonable to postulate its existence and estimate its magnitude. It is not feasible to determine anything definitive about any specific data that are collected with a UAV-thermal sensor from the results presented herein. To the best of the authors' knowledge, there are no methods for identifying or correcting for these errors using UAV-derived thermal images alone.

Given that there is the potential for thermal distortion in UAV thermal T_c meas-

urements and that the distortion is difficult to detect and quantify, efforts to reduce the distortion could prove useful. The data show relationships among the flight duration, measurement area, and thermal distortion for representative UAV-thermal missions (**Figure 8**). These data demonstrate that the magnitude of the thermal anomaly increases with flight duration, a trend that is evident across the range of irrigation treatments; however, the magnitude of the thermal anomaly decreases with increasing irrigation volume. The thermal distortions associated with the artificial UAV-thermal methods indicate that the identification of irrigation treatment differences with UAV-derived thermal data may be limited compared to fixed-IRT methods. As the number of measurements decreased, the ability to resolve irrigation treatment differences was negatively affected. The smaller number of T_c comparisons from a longer period between measurements would be compounded by the thermal distortion associated with UAV-thermal system that creates spurious differences among treatments.

There are several ways to reduce the effects of UAV-thermal distortion. Since the T_c is constantly changing during the period of measurement, the flight duration is the only parameter that can be controlled. Reduced flight duration is the most direct means to reduce UAV-thermal distortion. While decreasing the flight duration will reduce the thermal distortion, it will also reduce the area that can be measured (see **Figure 8**). In small plot studies the reduction of plot size can be accomplished but as the number of entities to measure increases, UAV-thermal imaging will become more complex. Increasing the imaging height will increase the area/image but may reduce the thermal and spatial resolution. Plot layout design with the temporal artifact in mind should be considered. The coincidence of increased image area and increased UAV-thermal distortion is potentially complex in large field studies. Field variability, e.g., soil type, irrigation efficiency, is often mitigated through replication. Replication increases plot area that in turn requires a larger study area. It is possible that under certain conditions the increased resolution achieved through replication would be offset by increased error in the thermal measurements. In such an instance, the potential improvements associated with increased reps should be considered due to the associated distortion of the thermal data resulting from increase study area. Finally, the inclusion of control plots with known thermal properties might prove useful though such mitigation is beyond the scope of this paper.

One of the most important considerations of this study was to determine the accuracy of thermal orthomosaic derived from imagery collected by a UAV. The ability to assemble individual UAV-thermal images into orthomosaic representations of T_c within a study area is a potential strength of UAV-thermal methods. Composite images are created by spatially aligning individual images into a mosaic image. Orthomosaic field representations from UAVs have proven useful in phenotyping crop characteristics such as plant density, ground cover, flowers, canopy height, and a host of others. However, T_c changes continuously over short time periods; thus, while images from a UAV-thermal system can be spatially

composited, a temporal thermal distortion is inherent in the resulting orthomosaic representations.

While use of UAV-derived thermal data on orthomosaic representations has inherent limitations, T_c data that are extracted from individual UAV images are likely useful in the detection of water use differences. The drawback of such imaging is that the spatial coverage is limited by the field of view of the thermal sensor and the altitude of the UAV when an image is collected. The balance between spatial coverage and thermal fidelity of UAV-thermal methods should be informed by knowledge of the thermal distortion that may occur. The data presented in this study should be sufficient to demonstrate UAV-thermal distortion. Users should be aware of these limitations when collecting thermographic data using UAV.

5. Conclusions

Based on comparisons of fixed-IRT and artificial UAV-thermal data presented here, several key conclusions are drawn. A UAV-thermal sensor distorts T_c values relative to those collected with a fixed-IRT. Additionally, the number of measurements that can be made using a UAV-thermal drone is limited compared to that of a fixed-IRT system, and the ability to differentiate T_c related to irrigation treatments is reduced. The combination of thermal distortion and reduced measurement frequency alters the number and pattern of irrigation treatment differences that can be detected using T_c. The temporal distortion can result in spurious treatment differences that diminish the utility of T_c as a tool for assessing differences in water deficit effects. While improving the spatial resolution, a UAV platform creates multiple sources of error for T_c measurements due to temporal distortion. While 0.5˚C was chosen as the threshold for these examples, other values that are either lower or higher might also be used to evaluate the effect of cutoff filters on treatment separations. In summary, the results from our analysis using artificially generated UAV thermal data demonstrated that implementing thermal UAV must be accompanied by a method to correct for the temporal distortion.

Declarations

Mention of trade names or commercial products in this publication is solely for the purpose of providing specific information and does not imply recommendations or endorsement by the US Department of Agriculture. The USDA is an equal opportunity provider and employer.

Conflicts of Interest

The authors declare no conflicts of interest regarding the publication of this paper.

References

[1] Wanjura, D.F. and Mahan, J.R. (1994) Thermal Environment of Cotton Irrigated Using Canopy Temperature. *Irrigation Science*, **14**, 199-205. https://doi.org/10.1007/bf00190191

[2] Wanjura, D.F., Upchurch, D.R. and Mahan, J.R. (2005) Behavior of Temperature-Based Water Stress Indicators in Biotic-Controlled Irrigation. *Irrigation Science*, **24**, 223-232. https://doi.org/10.1007/s00271-005-0021-9

[3] Wanjura, D.F., Upchurch, D.R., Mahan, J.R. and Burke, J.J. (2002) Cotton Yield and Applied Water Relationships under Drip Irrigation. *Agricultural Water Management*, **55**, 217-237. https://doi.org/10.1016/s0378-3774(01)00175-5

[4] Wanjura, D.F., Upchurch, D.R. and Mahan, J.R. (1995) Control of Irrigation Scheduling Using Temperature-Time Thresholds. *Transactions of the ASAE*, **38**, 403-409. https://doi.org/10.13031/2013.27846

[5] Mahan, J.R., Burke, J.J., Wanjura, D.F. and Upchurch, D.R. (2005) Determination of Temperature and Time Thresholds for BIOTIC Irrigation of Peanut on the Southern High Plains of Texas. *Irrigation Science*, **23**, 145-152. https://doi.org/10.1007/s00271-005-0102-9

[6] Mahan, J.R., Conaty, W., Neilsen, J., Payton, P. and Cox, S.B. (2010) Field Performance in Agricultural Settings of a Wireless Temperature Monitoring System Based on a Low-Cost Infrared Sensor. *Computers and Electronics in Agriculture*, **71**, 176-181. https://doi.org/10.1016/j.compag.2010.01.005

[7] Berni, J.A.J., Zarco-Tejada, P.J., Sepulcre-Cantó, G., Fereres, E. and Villalobos, F. (2009) Mapping Canopy Conductance and CWSI in Olive Orchards Using High Resolution Thermal Remote Sensing Imagery. *Remote Sensing of Environment*, **113**, 2380-2388. https://doi.org/10.1016/j.rse.2009.06.018

[8] Zarco-Tejada, P.J., González-Dugo, V. and Berni, J.A.J. (2012) Fluorescence, Temperature and Narrow-Band Indices Acquired from a UAV Platform for Water Stress Detection Using a Micro-Hyperspectral Imager and a Thermal Camera. *Remote Sensing of Environment*, **117**, 322-337. https://doi.org/10.1016/j.rse.2011.10.007

[9] Gonzalez-Dugo, V., Zarco-Tejada, P., Nicolás, E., Nortes, P.A., Alarcón, J.J., Intrigliolo, D.S., *et al.* (2013) Using High Resolution UAV Thermal Imagery to Assess the Variability in the Water Status of Five Fruit Tree Species within a Commercial Orchard. *Precision Agriculture*, **14**, 660-678. https://doi.org/10.1007/s11119-013-9322-9

[10] Tsouros, D.C., Bibi, S. and Sarigiannidis, P.G. (2019) A Review on UAV-Based Applications for Precision Agriculture. *Information*, **10**, Article 349. https://doi.org/10.3390/info10110349

[11] Messina, G. and Modica, G. (2020) Applications of UAV Thermal Imagery in Precision Agriculture: State of the Art and Future Research Outlook. *Remote Sensing*, **12**, Article 1491. https://doi.org/10.3390/rs12091491

[12] Maes, W., Huete, A. and Steppe, K. (2017) Optimizing the Processing of UAV-Based Thermal Imagery. *Remote Sensing*, **9**, Article 476. https://doi.org/10.3390/rs9050476

[13] Zhang, C. and Kovacs, J.M. (2012) The Application of Small Unmanned Aerial Systems for Precision Agriculture: A Review. *Precision Agriculture*, **13**, 693-712. https://doi.org/10.1007/s11119-012-9274-5

[14] Colomina, I. and Molina, P. (2014) Unmanned Aerial Systems for Photogrammetry and Remote Sensing: A Review. *Journal of Photogrammetry and Remote Sensing*, **92**, 79-97. https://doi.org/10.1016/j.isprsjprs.2014.02.013

[15] Raeva, P., Šedina, J. and Dlesk, A. (2018) UAV Photogrammetry Techniques for Precision Agriculture. *Proceedings of 7th International Conference on Cartography and GIS*, Sozopol, 18-23 June 2018, 842-856.

[16] Weiss, M., Jacob, F. and Duveiller, G. (2020) Remote Sensing for Agricultural Appli-

cations: A Meta-Review. *Remote Sensing of Environment*, **236**, Article 111402. https://doi.org/10.1016/j.rse.2019.111402

[17] Evett, S.R. (2015) Soil Water and Monitoring Technology. In: *Agronomy Monographs*, American Society of Agronomy, Crop Science Society of America and Soil Science Society of America, 23-84. https://doi.org/10.2134/agronmonogr30.2ed.c2

[18] Lascano, R.J. (2015) The Soil-Plant-Atmosphere System and Monitoring Technology. In: *Agronomy Monographs*, American Society of Agronomy, Crop Science Society of America and Soil Science Society of America, 85-115. https://doi.org/10.2134/agronmonogr30.2ed.c3

[19] Subedi, A. and Chávez, J.L. (2015) Crop Evapotranspiration (ET) Estimation Models: A Review and Discussion of the Applicability and Limitations of ET Methods. *Journal of Agricultural Science*, **7**, 50-68. https://doi.org/10.5539/jas.v7n6p50

[20] Howell, T.A., McCormick, R.L. and Phene, C.J. (1985) Design and Installation of Large Weighing Lysimeters. *Transactions of the ASAE*, **28**, 106-112. https://doi.org/10.13031/2013.32212

[21] Howell, T.A., Schneider, A.D., Dusek, D.A., Marek, T.H. and Steiner, J.L. (1995) Calibration and Scale Performance of Bushland Weighing Lysimeters. *Transactions of the ASAE*, **38**, 1019-1024. https://doi.org/10.13031/2013.27918

[22] Sakuratani, T. (1981) A Heat Balance Method for Measuring Water Flux in the Stem of Intact Plants. *Journal of Agricultural Meteorology*, **37**, 9-17. https://doi.org/10.2480/agrmet.37.9

[23] Jensen, M.E. (1968) Water Consumption by Agricultural Plants. In: *Water Deficits in Plant Growth*, Academic Press, 1-22.

[24] Lascano, R.J. (2000) A General System to Measure and Calculate Daily Crop Water Use. *Agronomy Journal*, **92**, 821-832. https://doi.org/10.2134/agronj2000.925821x

[25] Apogee Instruments (2024) The ASCE Standardized Reference Evapotranspiration Equation. https://www.apogeeinstruments.com/content/EWRI-ASCE-Reference-ET-Appendices.pdf

[26] Jackson, R.D., Idso, S.B., Reginato, R.J. and Pinter, P.J. (1981) Canopy Temperature as a Crop Water Stress Indicator. *Water Resources Research*, **17**, 1133-1138. https://doi.org/10.1029/wr017i004p01133

[27] Jackson, R.D., Kustas, W.P. and Choudhury, B.J. (1988) A Reexamination of the Crop Water Stress Index. *Irrigation Science*, **9**, 309-317. https://doi.org/10.1007/bf00296705

[28] Mahan, J.R., Young, A.W. and Payton, P. (2015) Continuously Monitored Canopy Temperature as a Proxy for Plant Water Status. *American Journal of Plant Sciences*, **6**, 2287-2302. https://doi.org/10.4236/ajps.2015.614232

[29] Chang, A., Jung, J., Maeda, M.M., Landivar, J.A., Carvalho, H.D.R. and Yeom, J. (2020) Measurement of Cotton Canopy Temperature Using Radiometric Thermal Sensor Mounted on the Unmanned Aerial Vehicle (UAV). *Journal of Sensors*, **2020**, 1-7. https://doi.org/10.1155/2020/8899325

[30] Goebel, T., Young, A., Payton, P., Maeda, M., Lascano, R. and Mahan, J. (2023) Estimating Cotton Canopy Temperature Artifacts in UAV-Based Thermal Measurements. *Journal of Cotton Science*, **27**, 140-148. https://doi.org/10.56454/qxgw5065